

*Axillary lymph node staging in breast cancer: clinical value of single photon emission computed tomography-computed tomography (SPECT-CT) with  $^{99m}\text{Tc}$ -methoxyisobutylisonitrile*

**Sergey Nikolaevich Novikov, Pavel Ivanovich Krzhivitskii, Sergey Vasilevich Kanaev, Petr Vladimirovich Krivorotko, et al.**

**Annals of Nuclear Medicine**

ISSN 0914-7187

Ann Nucl Med

DOI 10.1007/s12149-014-0926-6



**Your article is protected by copyright and all rights are held exclusively by The Japanese Society of Nuclear Medicine. This e-offprint is for personal use only and shall not be self-archived in electronic repositories. If you wish to self-archive your article, please use the accepted manuscript version for posting on your own website. You may further deposit the accepted manuscript version in any repository, provided it is only made publicly available 12 months after official publication or later and provided acknowledgement is given to the original source of publication and a link is inserted to the published article on Springer's website. The link must be accompanied by the following text: "The final publication is available at [link.springer.com](http://link.springer.com)".**

# Axillary lymph node staging in breast cancer: clinical value of single photon emission computed tomography-computed tomography (SPECT-CT) with $^{99m}\text{Tc}$ -methoxyisobutylisonitrile

Sergey Nikolaevich Novikov · Pavel Ivanovich Krzhivitskii · Sergey Vasilevich Kanaev · Petr Vladimirovich Krivorotko · Nikolay Dmirievich Ilin · Ludmila Alexeevna Jukova · Olga Igorevna Ponomareva

Received: 11 August 2014 / Accepted: 3 November 2014  
© The Japanese Society of Nuclear Medicine 2014

## Abstract

**Objective** To determine diagnostic accuracy of SPECT, CT and SPECT-CT in axillary lymph node (LN) staging in breast cancer (BC).

**Methods** Sixty consecutive patients with primary operable T1-3N<sub>x</sub>M0 BC were included in this study. All patients underwent SPECT-CT examination on Symbia-T16 scanner which consists of dual-head gamma camera combined with 16 slices diagnostic CT. SPECT-CT acquisition started 10–15 min after i/v injection of 740–1,000 MBq of  $^{99m}\text{Tc}$ -MIBI. On CT images of axillary LN we analyzed following diagnostic signs: size (short axis more or less than 10 mm), shape (round or oval), cortical thickness and fat content (solid or with fat gate). Intensity of tracer uptake in axillary LN was classified as follows: grade (Gr) I—background, Gr II—slightly above background, Gr III—intense but below uptake in muscles, Gr IV—as high as in muscles. Histological examination of dissected LN was used as gold standard.

**Results** Various combinations of CT signs of axillary LN involvement demonstrated moderate diagnostic value with best results characterized by low (55 %) sensitivity (SEN), 97 % specificity (SP) and 83 % accuracy (AC). Intensive (Gr IV) uptake of  $^{99m}\text{Tc}$ -MIBI in axillary LN characterized by low (55 %) SEN, high (100 %) SP and moderate

(84 %) AC. Combination of CT and SPECT signs looks most promising especially when LN metastases were diagnosed in patients with enlarged solid LN or normal sized LN with Gr III-IV  $^{99m}\text{Tc}$ -MIBI uptake. In these cases, SEN was equal to 75 %, SP-90 %, AC-85 %, only one of 5 patients with false negative results had metastases in more than 2 LN.

**Conclusions** By combination of SPECT and CT data we can more accurately diagnose axillary LN invasion by breast cancer.

**Keywords** Breast cancer · Axillary metastases · SPECT-CT · Staging

## Introduction

A preoperative assessment of axillary lymph node (LN) status in patients with breast carcinoma (BC) is known as an important prognostic factor which plays significant role in the selection of optimal treatment strategy. Metastatic involvement of axillary LN is considered as the main indication for neoadjuvant (or adjuvant) chemotherapy. Furthermore, the presence or absence of clinical signs of LN invasion is an important factor to clarify the scope of upcoming surgery such as lymphadenectomy or biopsy of the sentinel LN.

Unfortunately, when analyzing the status of axillary LN, the diagnostic value of standard “morphological” modalities such as mammography (MG), computed tomography (CT) as well as ultrasonography (USG) remains insufficient: the sensitivity, specificity, and overall accuracy do not exceed 40–83, 70–89, and 72–80 %, respectively [1, 2]. The expectations for a significant improvement in accuracy with the help of functional imaging, such as positron

S. N. Novikov (✉) · P. I. Krzhivitskii · S. V. Kanaev · N. D. Ilin · L. A. Jukova · O. I. Ponomareva  
Department of Radiation Oncology and Nuclear Medicine,  
N.N. Petrov Institute Oncology, Leningradskaya 68,  
St Petersburg 197758, Russia  
e-mail: krokon@mail.ru

P. V. Krivorotko  
Surgery Department No 1, N.N. Petrov Institute Oncology,  
Leningradskaya 68, St Petersburg 197758, Russia

emission tomography (PET) and single photon emission computed tomography (SPECT), have failed [3]. However, taking into account the diversity of information obtained by morphological and functional diagnostic modalities, it is possible to assume that their combined use will improve the capabilities of detecting metastatic invasion of the regional LN in patients with BC. For example, a study we conducted earlier demonstrated that the combined use of data of USG and planar breast scintigraphy with  $^{99m}\text{Tc}$ -methoxyisobutylisonitrile (MIBI) significantly increases the sensitivity and specificity in detecting axillary LN metastases [4]. In this regard, special attention should be given to a new hybrid technology combining single photon emission computed tomography and computed tomography (SPECT-CT) that allow one to acquire both morphological and functional information about the changes in a particular localization and also to evaluate severity of diagnosed abnormalities [5, 6]. Thus, we undertook the present study to analyze diagnostic value of different SPECT, CT and SPECT-CT signs of axillary LN invasion by BC and to evaluate accuracy of hybrid imaging in axillary staging.

## Materials and methods

This single-center prospective study was approved by local Ethic committee (N.N. Petrov Institute of Oncology, reference 2012–02). Informed and signed consent was obtained from all patients. Study was performed in a group of 60 primary BC patients aged 32 to 73 year; all cases were histologically verified. A clinical and instrumental examination had been conducted from March 2012 to November 2013. At the beginning of the study, 47 females were scheduled for surgical treatment because of biopsy proven BC, and in 13 cases for verification of pathologic process in the breast. In accordance with the results of preoperative clinical and radiological examinations, the distribution of primary BC in stages was as follows: T1 in 26, T2 in 32, and T3 in 2 observations. The axillary LNs were palpable in 18 patients, 3 cases of which were considered as metastatic, and the others were of indeterminate origin. All patients within 1–3 weeks after SPECT-CT underwent operative treatment, including sentinel LN biopsy (24 patients) or standard axillary dissection (36 females). The scope of interventions was extended to axillary lymph node dissection in 4 patients with intraoperatively positive sentinel LN. In the remaining 36 cases, from 6 to 22 LN were removed during axillary lymphadenectomy.

The SPECT-CT examination was performed on hybrid camera (“Symbia T16”) which consists of dual head  $\gamma$ -camera with low-energy high-resolution collimators (LEHR) and diagnostic multislice (16-slices) spiral CT.

Image acquisition started 5–15 min after injection of 740–1,000 MBq of  $^{99m}\text{Tc}$ -MIBI into a vein in one of the feet. The upper bound of the scanning region was located at the upper third of the neck, and the lower one was 1–2 cm below the dome of the diaphragm. At the first stage, SPECT was performed with the following acquisition parameters:  $128 \times 128$  matrix; 3 degrees angular steps in 15 s time per frame; 60 frames for each detector. After completion of SPECT (without changing the patient's position on the table), spiral CT was performed (tube voltage, 100 kV; 80–100 mA; tube rotation time, 0.7–0.8 s; scan time, 10–15 s; slice thickness, 3 mm with reconstruction of 1 mm; pitch, 1 mm).

Processing of the obtained data was performed on a Syngo workstation (“Siemens”): the iterative reconstruction technique (iterations, 8; subsets, 16) with the mandatory attenuation correction was used for the scintigraphic data. CT images of the axillary LNs were obtained using the B 30–60 filters and analyzed in the soft tissue window. Total time of SPECT-CT scanning was about 20–25 min. Images were analyzed using 2-dimensional orthogonal reslicing in axial, sagittal and coronal directions in fused and separate (SPECT, CT) modes. The obtained SPECT-CT data were evaluated by nuclear medicine physician and radiologist whose professional experience was more than 10 years each. The radiologist analyzed the following LN parameters: shape (oval or round), size (along the short and long axis), and structure (presence or absence of the fatty hilus, cortical thickness). To conclude on axillary LN metastases, the following classical criteria were used: a round shape and an increase in size of the LN along the short axis (more than 10 mm), the solid structure of the LN (no fatty hilus), and uneven thickening of the LN cortical layer. The detected round LNs of the solid structure (without fatty hilus) up to 10 mm along the short axis were also regarded as affected.

At the next stage, nuclear medicine specialist analyzed the obtained SPECT images. In this case, he was provided with the results of the X-ray findings. The  $^{99m}\text{Tc}$ -MIBI accumulation rate in the LN projection was estimated according to the following semiquantitative classification: the first (I) grade was established at slight tracer accumulation not exceeding uptake in the surrounding fat tissue (background level); the second (II) grade was characterized by moderate  $^{99m}\text{Tc}$ -MIBI accumulation exceeding the background level, but less intense than uptake in the surrounding muscle structures; the third (III) grade was characterized by active, comparable to muscles, tracer uptake; the fourth (IV) grade was set at the maximum rate, at the level of  $^{99m}\text{Tc}$ -MIBI uptake in the surrounding muscle tissues or higher. The grades III and IV accumulation of  $^{99m}\text{Tc}$ -MIBI in the LN was considered as the main criteria for its metastatic invasion.

The same semiquantitative classification was used for characterization of  $^{99m}\text{Tc}$ -MIBI uptake in primary lesion. Grades I and II were considered as normal or nonspecific tracer uptake in breast. Grades III (moderate) and IV (marked tracer uptake) were determined as suspicious and highly suggestive for breast cancer. In addition we used semiquantitative index (T/B), which was presented by the following equation: average counts per pixel in region of interest drawn around tumor divided by average count per pixel in adjacent background region in the same breast.

A combined analysis of the SPECT-CT data was started with searching for foci of increased tracer accumulation on SPECT scans with parallel anatomical comparison on CT images. Intense  $^{99m}\text{Tc}$ -MIBI uptake was most often observed in the vascular walls, muscles, or affected LNs. Additionally, the tomograms were subjected to the targeted search for the axillary LN and analysis for the grade of tracer accumulation in them.

The results of a subsequent histopathological study were used for verification of diagnostic data and calculations of sensitivity, specificity and overall accuracy of various diagnostic signs and their combinations. Statistical processing of the obtained data was performed using a standard Statistica 6.0 software package.

## Results

A histological examination revealed axillary LN metastases in 20 (33 %) of the 60 examined patients. They were most often detected in patients after standard LN dissection (17 cases) and less often after sentinel LN biopsy or limited lymphadenectomy (3 cases). It is noteworthy that extensive involvement of axillary LN (3 or more affected LN) was mentioned only in 8 of the 20 patients with axillary metastases. Metastatic invasion of one or two LN was detected in 12 cases.

According to CT data, an enlargement (more than 10 mm on short axis) of the axillary LN was mentioned in 20 of the 60 examined patients. Of these, metastases were confirmed histopathologically only in 12 cases, the remaining 8 patients had nonspecific changes in LN. On the contrary, in another 8 patients the presence of histopathological signs of LN involvement by BC was not associated with enlarged LN (Fig. 1). As a result, enlargement of axillary LN was characterized by a low sensitivity (60 %) and moderate specificity (80 %). The use of other radiological criteria of metastatic LN involvement, the LN solid structure in combination with the lack of fatty hilus, enabled the achievement of a significant increase in the specificity (90 %): the solid structure was determined in 15 patients and in 11 cases malignant nature of these changes was confirmed by pathology. Taking into account the high

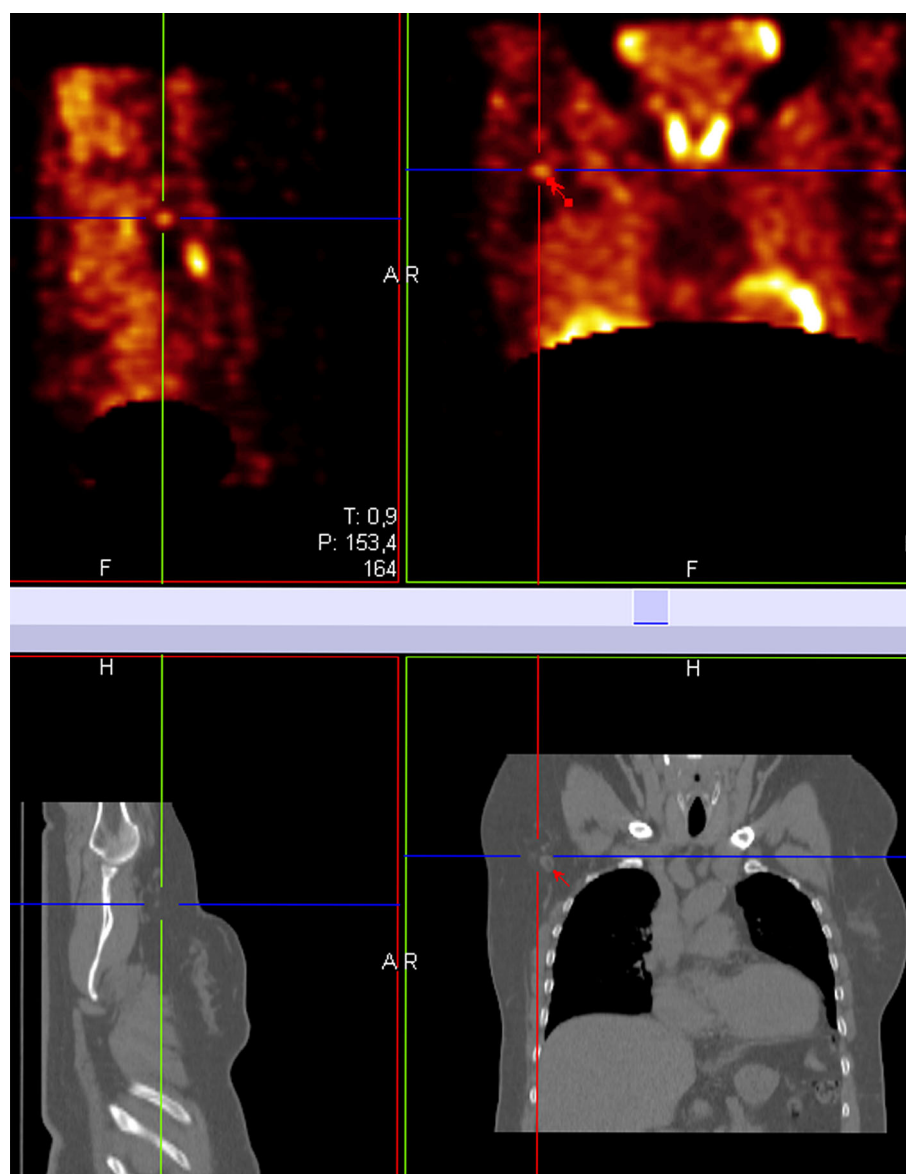
specificity of this sign, we analyzed diagnostic accuracy of combined criteria which was characterized by the presence of the solid structure and size of the axillary LN. For example, the combination of enlarged size and solid structure of the axillary LN was found in 12 patients. Histological examination confirmed the presence of metastatic invasion in 11 of them regardless of the LN shape. The false positive result was identified only in 1 case. Despite a relatively low sensitivity (55 %), combination of this signs has a high specificity (97 %) and overall accuracy (83 %). It should be noted that the LN of the oval shape with the well-defined fatty hilus and maximum size of less than 7 mm along the short axis were detected on CT images in 8 patients with histologically verified involvement of the axillary LN by BC. An enlargement of the LN with preserving the shape and structure was accompanied by the verified metastatic lesions only in 1 of 6 cases.

An analysis of the SPECT data revealed intense (grade IV)  $^{99m}\text{Tc}$ -MIBI accumulation in the axillary LN in 11 of the 60 patients, with metastases being confirmed in all of them (Fig. 2). The sensitivity, specificity, and accuracy upon the use of this sign as a criterion for a LN invasion were 55, 100, and 85 %, respectively. In cases where the presence of grades III and IV tracer accumulation in the LN was considered as a sign of metastatic lesion, the sensitivity, specificity, and overall accuracy were 75, 85, and 82 %, respectively.

In addition, we analyzed the capabilities of the concomitant use of various combinations of the anatomical and functional signs of a metastatic lesion of the axillary LN in the studied patients (Table 1). It turned out that if axillary LN metastases are detected in the presence of enlarged LN without fatty hilus or non-enlarged LN with or without fatty hilus, but with intense (grade IV)  $^{99m}\text{Tc}$ -MIBI uptake, the sensitivity of diagnostic conclusions is 65 %, with the specificity and overall accuracy being 97 and 87 %, respectively. If metastases in non-enlarged LN were detected in the presence of the grades III-IV  $^{99m}\text{Tc}$ -MIBI hyperfixation, the sensitivity of diagnostic results was increased to 75 % due to a reduction in the specificity (90 %) and a slight decline in the overall accuracy (85 %). It should be emphasized that when we used the last combination of pathologic signs in 4 of 5 patients with false negative SPECT-CT conclusions histopathological examination revealed only one or two involved LN. This fact gives us opportunity to propose that only about 6 % of cases with extensive LN invasion outside sentinel LN would be missed by SPECT-CT.

We didn't find any significant relationship between  $^{99m}\text{Tc}$ -MIBI uptake in the primary tumor and accuracy of SPECT and SPECT-CT diagnosis of axillary LN metastases.  $^{99m}\text{Tc}$ -MIBI SPECT-CT detected focal lesions with moderate or marked increase in tracer accumulation in

**Fig. 1** A 57-year-old female with breast cancer. SPECT shows increased accumulation of  $^{99m}\text{Tc}$ -MIBI in the axillary lymph node, which was histologically diagnosed as metastatic (arrow). CT demonstrates no significant lymphadenopathy



56/60 patients; in 4/60 cases BC lesions were negative. All 4 women with non-visualized primary tumor had small (less than 10 mm) BC without signs of axillary lymph node involvement on SPECT-CT, SPECT, CT and according to postoperative histological examinations.

The values of T/B index in primary tumors of 5 patients with false negative SPECT-CT conclusions about status of axillary LN [average 3.46 (1.7–4.8)] and remaining 55 patients [average 3.51 (1.4–7.1)] were identical.

## Discussion

Computed tomography and ultrasonography are known as the basic methods for the diagnosis of axillary LN involvement in patients with BC. LN enlargement of more

than 10 mm along the short axis is used as the main CT sign of metastatic invasion. The shape changes and structure disturbances of the LN as well as nonuniform changes in the cortical layer thickness are determined as important additional sign of LN metastases. Our findings confirm their diagnostic value. This is, in particular, confirmed by the high specificity (97 %) in the detection of the enlarged axillary LN lacking the fatty hilus. However, the low sensitivity of CT, which did not exceed 55 % in this study upon using any criteria, does not allow to recommend it as a routine examination for diagnosis of axillary LN invasion. This conclusion is almost completely consistent with the literature data. For example, a meta-analysis of the 16 largest studies demonstrated that the sensitivity of any X-ray diagnostic criteria used to detect BC metastases in the LNs varies from 44 to 71 % [7].

**Fig. 2** The enlarged LN with the solid structure (without fatty hilus) and intense (grade IV) tracer uptake. Metastatic involvement is confirmed by biopsy

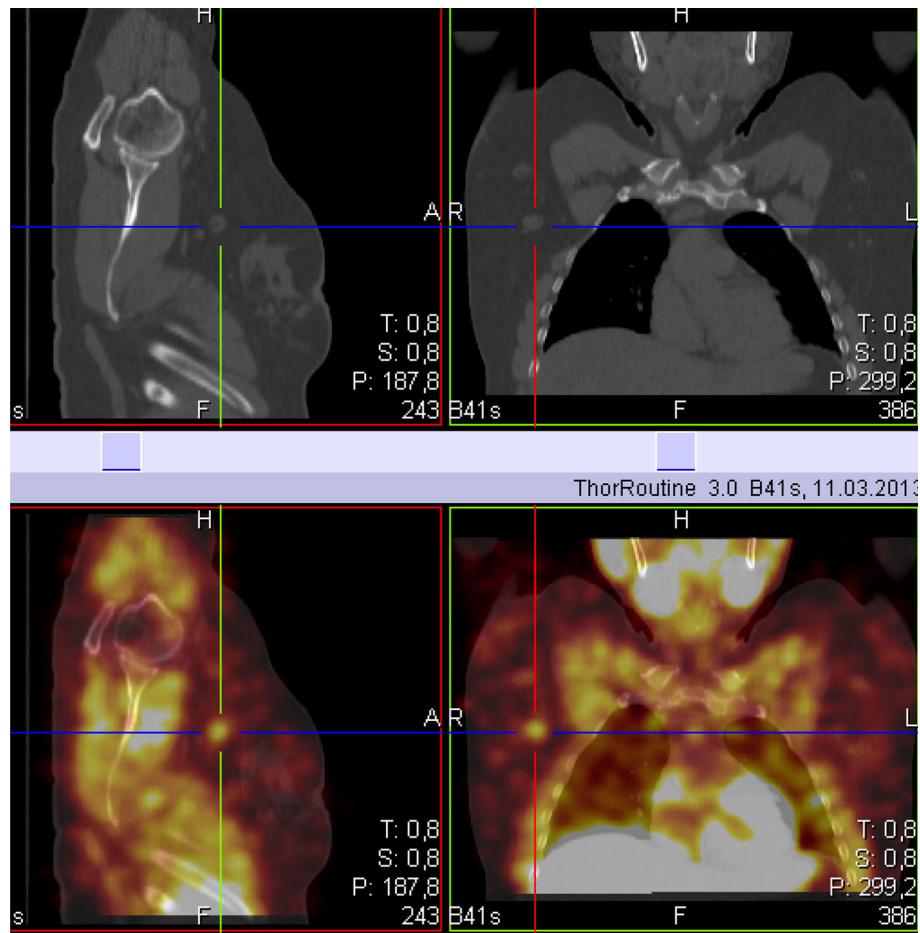


**Table 1** Diagnostic value of different SPECT-CT pathological signs and their combinations in detecting axillary metastases

	Modality, diagnostic signs or their combination					
	CT enlarged LN without fat gate	CT enlarged LN	SPECT grades III–IV tracer uptake	SPECT grade IV tracer uptake	SPECT-CT combination 1 <sup>a</sup>	SPECT-CT combination 2 <sup>b</sup>
Sensitivity	55 % (11/20)	60 % (12/20)	75 % (15/20)	55 % (11/20)	65 % (13/20)	75 % (15/20)
Specificity	97 % <sup>''</sup> (39/40)	80 % <sup>''</sup> (32/40)	85 % <sup>'''</sup> (34/40)	100 % <sup>''</sup> (40/40)	97 % <sup>''</sup> (39/40)	90 % (36/40)
Accuracy	83 % (50/60)	73 % <sup>†</sup> (44/60)	82 % (49/60)	85 % <sup>†</sup> (51/60)	87 % <sup>††</sup> (52/60)	85 % (51/60)

SPECT single photon emission computed tomography, CT computed tomography, SPECT-CT single photon emission computed tomography-computed tomography, LNs lymph nodes

<sup>a</sup> Combination 1 axillary metastases were diagnosed by SPECT-CT if enlarged LN without fatty hilus were revealed on CT or intense (grade IV) 99mTc-MIBI uptake was detected in non-enlarged axillary LN

<sup>b</sup> Combination 2 axillary metastases were diagnosed by SPECT-CT if enlarged LN without fatty hilus were revealed on CT or grades III–IV 99mTc-MIBI uptake was detected in non-enlarged axillary LN

<sup>''</sup>Statistically significant differences in specificity,  $p = 0.01$  (<sup>''</sup>) and  $p = 0.03$  (<sup>'''</sup>)

<sup>†</sup>Statistically significant differences in accuracy,  $p = 0.04$  (<sup>††</sup>) and  $p = 0.05$  (<sup>†</sup>)

Diagnosis of primary tumors as well as metastatic lesions by methods of functional imaging (SPECT and PET) is based on different principles for the detection of malignant changes that are determination of the tumor cell metabolic activity and/or an increase in the expression of tumor-specific targets (receptors, antigens, enzymes, etc.).

The most common and well-known functional method of imaging in oncology is PET with a labeled glucose analog, 18-F-fluoro-2-deoxy-D-glucose (FDG). An increase in the glucose metabolic activity in tumor cells results in intense accumulation of the glucose analog, FDG, and effective visualization of lesions. Preliminary data indicated the

extremely high accuracy of PET in the diagnosis of metastatic involvement of the regional LN in patients with BC: reported values of sensitivity, specificity, and overall accuracy amounted to 94–100, 86–100, and 89–92 %, respectively [8]. However, a later comparative analysis of PET with FDG and the sentinel LN biopsy revealed a low sensitivity (20–61 %) of PET in detecting subclinical (few millimeters) metastatic invasion of the axillary LN [9].

In terms of the basic principles of the functional imaging of BC lesions, SPECT with tumor  $^{99m}\text{Tc}$ -MIBI can be considered as low cost substitute of FDG PET. Tumor visualization with  $^{99m}\text{Tc}$ -MIBI is based on the phenomenon of increased mitochondrial uptake of lipophilic cations (MIBI, tetrofosmin) labeled with  $^{99m}\text{Tc}$  in metabolically active tumor cells. Taking into account the fact that the metabolic changes usually precede anatomical rearrangement, “functional imaging” is assumed to possess a higher sensitivity in the diagnosis of both primary and secondary neoplastic changes. The first experience with the use of  $^{99m}\text{Tc}$  labeled lipophilic cations for the detection of LN metastases in patients with BC brought some disappointment because the sensitivity and specificity of these studies in a planar mode were lower than the expected values and did not exceed 41–79 % [10]. The main reason for this low sensitivity was a low resolution of standard planar nuclear medicine examinations. Improvements in instrumental basis and the introduction of SPECT technology promoted the revival of interest in the use of scintigraphy for the diagnosis of the regional LN metastases in patients with BC. A detailed review by Madeddu and Spanu [5] demonstrated that the use of SPECT having a higher resolution than that of planar radionuclide imaging techniques led to a substantial increase in the sensitivity and specificity. For example, in 2 large European studies [11–13], which included the data of 277 patients that underwent SPECT examinations, the sensitivity, specificity, and overall accuracy of the diagnosis of axillary LN metastases reached 87–94, 92–93, and 90–92 %, respectively.

Our own experience with the use of  $^{99m}\text{Tc}$  labeled lipophilic cations for the diagnosis of metastatic changes in the axillary LN in 168 patients with BC indicates the more modest capabilities of SPECT: the sensitivity, specificity, and overall accuracy were 71, 76, and 74 %, respectively [4]. Similar results were obtained by other authors [14]. As possible causes of this variability, the differences in clinical characteristics of examined patients, modes of image acquisition, reconstruction, and interpretation criteria's may be considered. In our view, the most significant difficulties in analysis of SPECT data are associated with uneven tracer accumulation in the area of interest: uptake in the affected LN as well as in the neighbor blood vessels and muscles. It may be assumed that the use of hybrid SPECT-CT technology that provides the exact anatomical

localization of tracer accumulation and a thorough evaluation of the rate of  $^{99m}\text{Tc}$ -MIBI uptake in them will increase the sensitivity and specificity of detection of the metastatic LN. The presented preliminary data indicate the increased diagnostic accuracy and incremental value of SPECT-CT over CT, planar scintigraphy, and SPECT. An important outcome of the presented study is the development of combined anatomical and functional signs of the metastatic axillary LN invasion that allow improvement in interpretation of diagnostic data and provide the 94 % sensitivity in cases of extensive (more than 2 LN) LN involvement.

All of the above leads to the following conclusions. Combined functional and morphological information provided by SPECT-CT enables a significant increase in the diagnostic value of noninvasive detection of the axillary LN invasion by BC: the sensitivity of SPECT-CT is increased by 1.4 times (from 55 to 75 %) compared with CT, with excellent specificity (97 and 89 %) and comparable overall accuracy (82 and 84 %). The sensitivity of SPECT-CT for the diagnosis of extensive (3 or more LN) involvement of the axillary LN in BC patients is very promising with only one missed lesion, which allows us to recommend the use of SPECT-CT as a mandatory method for the selection of patients for limited lymph node dissections or sentinel LN biopsy. The combination of morphological (enlargement and solid structure of the LN) and functional (grades III-IV IA accumulation rate) information provides the highest efficacy of the diagnosis of axillary LN metastases, which exceeds the diagnostic capabilities of each method apart.

**Conflict of interest** The authors declare that they have no conflict of interests.

## References

1. Mathijssen IM, Strijdhorst H, Kiestra SK, Wereldsma JC. Added value of ultrasound in screening the clinically negative axilla in breast cancer. *J Surg Oncol*. 2006;94:364–7.
2. Zgajnar J, Hocevar M, Podkrajsek M, Hertl K, Frkovic-Grazio S, Vidmar G, et al. Patients with preoperatively ultrasonically uninvolved axillary lymph nodes: a distinct subgroup of early breast cancer patients. *Breast Cancer Res Treat*. 2006;97:293–9.
3. Peare R, Staff RT, Heys SD. The use of FDG-PET in assessing axillary lymph node status in breast cancer: a systematic review and meta-analysis of the literature. *Breast Cancer Res Treat*. 2010;123:281–90.
4. Kanaev SV, Krivorotko PV, Novikov SN, Semiglazov VF, Semiglazova TYu, Turkevich EA, et al. Combination of scintigraphy with  $^{99m}\text{Tc}$ -MIBI and US in diagnosis of axillary lymph node metastases in patients with breast cancer. *Vopr Onkol (rus.)*. 2013;59:59–64.
5. Madeddu G, Spanu A. Use of tomographic nuclear medicine procedures, SPECT and pinhole SPECT, with cationic lipophilic radiotracers for the evaluation of axillary lymph node status in

- breast cancer patients. *Eur J Nucl Med Mol Imaging*. 2004; 31(suppl 1):23–34.
6. Mariani G, Bruselli L, Kuwert T, Kim EE, Flotats A, Israel O, et al. Review on the clinical uses of SPECT/CT. *Eur J Nucl Med Mol Imaging*. 2010;37:1959–85.
  7. Alvarez S, Anorbe E, Alcorta P, Lopez F, Alonso I, Cortes J. Role of sonography in the diagnosis of axillary lymph node metastases in breast cancer: a systematic review. *Am J Roentgenol*. 2006; 186:1342–8.
  8. Crippa F, Gerali A, Alessi A, Agresti R, Bombardieri E. FDG-PET for axillary node staging in primary breast cancer. *Eur J Nucl Med Mol Imaging*. 2004;31(suppl 1):97–102.
  9. Wahl R, Stegel BA, Coleman RE, Gatsonis CG. Prospective multicenter study of axillary nodal staging by positron emission tomography in breast cancer: a report of the staging breast cancer with PET study group. *J Clin Oncol*. 2004;22:277–85.
  10. Buscombe JR, Cwikla JB, Thakrar DS, Hilson AJW. Scintigraphic imaging of breast cancer: a review. *Nucl Med Commun*. 1997;18:698–709.
  11. Schillaci O, Scopinaro F, Spanu A, Donnetti M, Danieli R, Di Luzio E, et al. Detection of axillary lymph node metastases in breast cancer with Tc-99m tetrofosmin scintigraphy. *Int J Oncol*. 2002;20:483–7.
  12. Spanu A, Tanda F, Dettori G, Manca A, Chessa F, Porcu A, et al. The role of 99mTc-tetrofosmin pinhole-SPECT in breast cancer non-palpable axillary lymph node metastases detection. *Q J Nucl Med*. 2003;47:116–28.
  13. Taillefer R. Clinical applications of 99mTc-sestamibi scintigraphy. *Semin Nucl Med*. 2005;35:100–15.
  14. Tiling R, Tatsch K, Sommer H. Technetium-99m-sestamibi scintimammography for the detection of breast carcinoma: comparison between planar and SPECT imaging. *J Nucl Med*. 1998;39:849–56.